

Measurements of partially spatially coherent laser beam intensity fluctuations propagating through a hot-air turbulence emulator and comparison with both terrestrial and maritime environments

C. Nelson^{*a,d}, S. Avramov-Zamurovic^a, O. Korotkova^b, R. Malek-Madani^a, R. Sova^c, F. Davidson^d

^aThe United States Naval Academy, 121 Blake Road, Annapolis, MD 21402, USA

^bThe University of Miami, 1320 Campo Sano Drive, Coral Gables, FL, 33146 USA

^cThe Johns Hopkins University Applied Physics Laboratory, 11100 Johns Hopkins Road, Laurel, MD 20723, USA

^dThe Johns Hopkins University, 3400 N. Charles Street, Baltimore, MD 21218, USA;

Measurements of partially spatially coherent infra-red laser beam intensity fluctuations propagating through a hot-air turbulence emulator are compared with visible laser beam intensity fluctuations in the maritime and IR laser beam intensity fluctuations in the terrestrial environment at the United States Naval Academy. The emulator used in the laboratory for the comparison is capable of generating controlled optical clear air turbulence ranging from weak to strong scintillation. Control of the degree of spatial coherence of the propagating laser beam was accomplished using both infra-red and visible spatial light modulators. Specific statistical analysis compares the probability density and temporal autocovariance functions, and fade statistics of the propagating laser beam between the in-laboratory emulation and the maritime field experiment. Additionally, the scintillation index across varying degrees of spatial coherence is compared for both the maritime and terrestrial field experiments as well as the in-laboratory emulation. The possibility of a scintillation index ‘sweet’ spot is explored.

Keywords: Free-space optical communications, atmospheric turbulence, hot-air turbulence emulator, partial spatial coherence, maritime

1. INTRODUCTION

A laser beam propagating in a maritime environment can experience significant intensity fluctuations due to optical turbulence along the propagation path, resulting in high bit-error rates (BER) [1]. Understanding how to effectively mitigate some of the intensity fluctuations can be critical to the performance of an optical communication system. Additionally, being able to experiment in a controlled laboratory setting capable of simulating some of the scaled effects of the environment holds great advantages in cost, testing methods, and optimization.

This paper focuses on the first and second order statistics of the propagating laser beam. Specific statistical analysis compares the probability density and temporal autocovariance functions, and fade statistics of the propagating laser beam between the in-laboratory emulation and the maritime field experiment. Additionally, the scintillation index across varying degrees of spatial coherence is compared for both the maritime and terrestrial field experiments as well as the in-laboratory emulation. The possibility of a scintillation index ‘sweet’ spot is explored. The PDF of the intensity for a given detector is critical for estimation of the fade statistics of an optical signal, the temporal autocovariance function may provide fundamental insight into the length and depth of

*cnelson@usna.edu; phone 410-293-6164; fax 443-778-0619; www.usna.edu

fades through a single exponential fit correlation time, and optimization of the scintillation index through control of the degree of spatial coherence may lead to optimization of the BER.

Recent in-laboratory theory and experimentation has been done on partially spatially coherent laser beam propagation by Drexler et.al. [2], but we are aware of very little testing and experimentation in the field using partial spatial coherence for infra-red (IR) and Helium Neon (HeNe) laser beam propagation.

2. THEORETICAL BACKGROUND

The theoretical foundation used in this proposal was recently formulated in references [3, 4]. Specifically, the PDF, W , of the fluctuating intensity, I , gives the probability that the beam's intensity attains a certain level as described in the following equations where the intensity is normalized by its mean value.

$$Probability(a < I < b) = \int_a^b W(I) dI \quad (1)$$

The PDF can be reconstructed from measured intensities by using the statistical moments. The statistical moments are obtained using the following formula:

$$\langle I^{(n)} \rangle = \int_0^\infty W(I) I^n dI \quad (2)$$

Several PDF models have been suggested for light propagation in random media. We investigate two models, the Gamma-Laguerre [4, 5], and the Lognormal [6] PDF models. Note, the turbulence level in the field experiments and in laboratory hot-air turbulence emulator runs for this paper were too low to fit the most commonly used PDF model, the Gamma-Gamma [7].

As discussed in [3] and repeated here for clarity, in addition to PDF models for the optical propagation we make comparison of the temporal 2nd order autocovariance function expressed as follows [8]:

$$B_x(t_1, t_2) = \langle [x(t_1) - \langle x(t_1) \rangle][x(t_2) - \langle x(t_2) \rangle] \rangle \quad (3)$$

For a stationary process the temporal autocovariance function becomes: $B_x(\tau) = R_x(\tau) - m^2$ where $\tau = t_2 - t_1$, $R_x(\tau) = \langle x(t_1)x(t_2) \rangle$ is the correlation function, and m is the mean of the log-irradiance intensity. For this work, $x(t_1)$ and $x(t_2)$ represent the log-irradiance values at time t_1 and t_2 respectively.

Through the temporal autocovariance function, the decay constant, T_I , or typical correlation time of a single exponential fit may give us additional insight and information about the duration and frequency of fades which are critical for free-space optical communication (FSO) system performance. The single exponential fit to the temporal autocovariance function was accomplished through MATLAB's FMINSEARCH [9] function and the general form used for the exponential function is as follows:

$$B_{(exp\ fit)}(t_{data}) = Ae^{(-t_{data}/T_I)} \quad (4)$$

where T_I is referred to as the correlation time, or 1/e point for the single exponential, t_{data} is time of the data, and A is the value at $t_{data} = 0$.

Recent theory developed by Jennifer Ricklin and Frederic Davidson [10, 11] on the use of a spatially partially coherent source beam as applied to atmospheric turbulence for the communication channel shows that by reducing the spatial coherence of the propagating laser beam in certain cases the scintillations will decrease at the receiver, thereby improving the BER.

Experimental implementation of this theory has been accomplished using a spatial light modulator (SLM) for both visible and infra-red (IR) frequencies. A spatial light modulator allows direct control over the phase of the laser beam. Specifically, phase screens used to generate a Gaussian Schell Model beam have been developed in MATLAB for implementation with the SLMs utilizing theory by Shirai, Korotkova, and Wolf in their paper, “A method of generating electromagnetic Gaussian Schell-model beams,” [12]. See Figure 1 for sample phase screens produced and as used in our experiments.

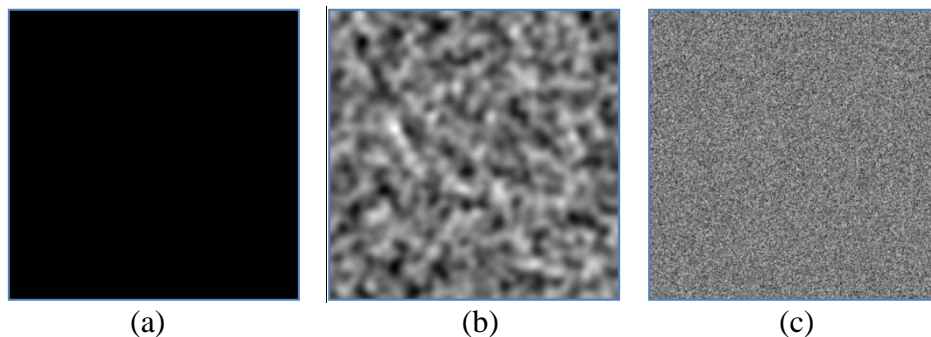


Figure 1 – γ_ϕ^2 in units of (pixels²) – a) Black (Coherent), b) $\gamma_\phi^2 = 128$, c) $\gamma_\phi^2 = 1$ (Strong Diffuser)

SLM phase screen values, i.e. a value of 128, relate the approximate squared value of the size of the speckle (approximate size of speckle – γ_ϕ) in number of pixels. This is the correlation width (γ_ϕ^2) squared value of the Gaussian window function used to produce the phase screen as outlined in [12]. More generally, Black (Figure 1a), or constant phase, describes fully coherent laser beam propagation, where a value of 1 (Figure 1c) corresponds to nearly incoherent laser beam propagation or the effects of a strong diffuser. For the case of 128 (more weakly diffusing), the approximate speckle size, γ_ϕ is computed as follows: The SLM array has 512 x 512 pixels over 7.68 mm by 7.68

mm and so $\gamma_\phi = \frac{7.68mm}{512} \times \sqrt{128} = 0.17$ mm.

3. EXPERIMENT DESCRIPTION AND LABORATORY COMPARISON

Figure 2 illustrates the two field test set-ups used at USNA for comparison.



(a)



(b)

Figure 2 – USNA field tests, arrows show direction of laser beam propagation – (a) 180 m IR (1550 nm) laser beam propagation, scintillometer view is seen in left hand image, (b) 314 m HeNe (632.8 nm) laser beam propagation over creek. Left-hand side is the transmitter view, and the right-hand side image is the receiver side view. Scintillometer was aligned along beam path.

For the USNA field test, both an IR (1550 nm) and HeNe (632.8 nm) laser were used. The IR laser beam was used overland (Figure 2a) with a 180 m propagation distance, and the HeNe laser was used over the water (Figure 2b) with a 314 m propagation distance. In both experiments the laser beam was vertically polarized, went through a beam expander (IR and visible), reflected from a 7.68 mm x 7.68 mm SLM (IR and visible) and then propagated through the atmosphere to a target receiver. At the receiver an amplified photodetector and data acquisition device were used to collect data at 10,000 samples/second. Each data run was approximately two minutes in duration. A scintillometer was used to estimate the value of C_n^2 over the propagation path for both field tests. C_n^2 was measured at $\sim 1 \cdot 10^{-14} \text{ m}^{-2/3}$ for the 314 m over the creek test (Figure 2b), and we believe the scintillometer may have been misaligned during the 180 m terrestrial test (Figure 2a) and therefore C_n^2 was estimated to be $\sim 10^{-15} \text{ m}^{-2/3}$ based on previous measurements.

The in laboratory hot-air turbulence emulator as described in [3] (Figure 3) and repeated here for clarity measures 91.4 cm (3 ft.) in length, and 15.2 cm in height and width (6 inches). The hot-air turbulence emulator is ‘broken’ up into 5 sections of equal distance where the first, second, fourth, and fifth positions are taken up in heat guns and variable speed fans. Ten K-type thermocouple probes were positioned ~3.8 cm apart on either side of the beam propagation path and connected to a data logger that collects temperature readings every 1 second. The heat guns provided thermal flow from one (red arrows in Figure 3a) side while fans provided ambient air counter flow (white arrows in Figure 3a). The air flows met in the middle and created a turbulent propagation channel which was then exhausted through section 3 (both directions). Additionally, four diffuser screens were placed between the heat gun exhaust and the propagation channel where heat gun positioning was done to maximize the temperature difference across the thermocouples.

For the in-laboratory simulation of the field test at USNA a distributed feedback (DFB) laser operating near 1550 nm was connected to a single-mode (SM) fiber, sent to a 1.6 mm diameter fiber collimator, vertically polarized, sent through an IR beam expander, and then reflected from a SLM with window dimensions of 7.68 x 7.68 mm. The SLM was set-up for constant phase modulation across the beam profile with no cycling of the phase screens – the SLM is limited to ~45 Hz cycling and this is too slow compared with the 10,000 samples of data collected/second. The beam then passed through a mechanical iris set at 3.5 mm diameter before passing through the hot-air turbulence emulator and on to an amplified photodetector with aperture area of 0.8 mm². The total propagation distance for the USNA simulation was 2 m and the mechanical iris was used to reduce the Fresnel Number, N_f , as computed from [13] to just below 1.0 (not fully far field). Note, the Fresnel Number of around 1 was higher than the Fresnel Number of the field experiment which was around 0.1 – further reduction of the mechanical iris diameter was avoided to minimize any effect on the spatial profile from the SLM.

The turbulence in the hot-air turbulence emulator was found to be approximately Kolmogorov along the beam propagation axis [3].

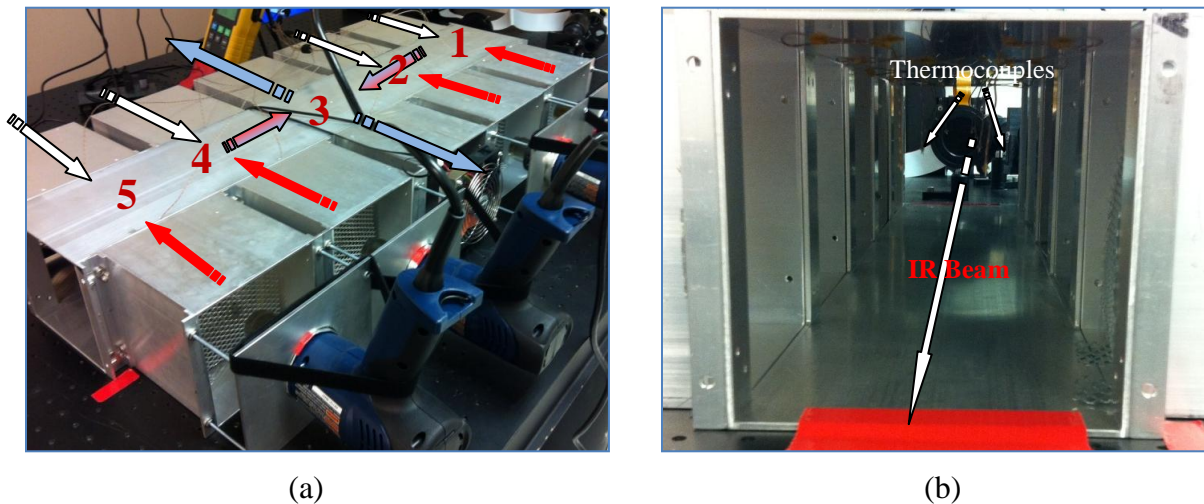


Figure 3 – Hot-air turbulence emulator experimental set-up – (a) air flow in turbulence emulator with sections labeled 1 through 5, (b) propagation channel with thermocouples (two of the ten identified by arrows)

4. RESULTS

The data plots in this section compare (1) the observed scintillation index, σ_I^2 , (2) temporal autocovariance functions through the correlation time, T_I , (3) approximated ratio of the source aperture diameter to spatial coherence radius, D_S/ρ_0 , where ρ_0 , is as computed from [8] and is used to scale the turbulence between atmosphere and laboratory (this is described in a number of papers, see [14] for one example), (4) the Fresnel Number, N_f , as computed from [15] and (5) fade statistics (number of fades, cumulative probability of fade, and channel availability) between field tests performed and the in-laboratory experiments utilizing a hot-air turbulence emulator. Additional PDF analysis of an IR laser beam propagating in a maritime environment can be found in [16] as well as in [4].

The fade statistics were computed by comparing the received intensity with an arbitrary threshold level set at 1 dB below the mean intensity value. Channel availability was computed by taking the number of intensity points above threshold and dividing this by the sum of the points above and below threshold.

Fig. 4 shows a representative figure for the cumulative probability of fade length (314 m HeNe over water case shown) for the experiments, where Tau, in seconds, is defined as the duration of the fade.

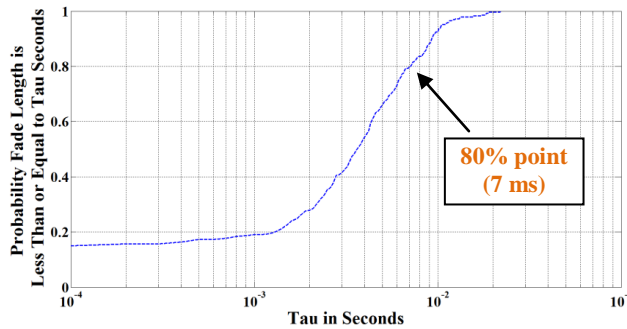


Figure 4 – Cumulative probability of fade for 314 m over creek field test for fully coherent (Black phase screen) laser beam propagation.

Table 1 summarizes the comparison of the over the water, HeNe field test with IR laser beam propagation through an in-laboratory hot-air turbulence emulator. Figures 5 and 6 show the PDFs and temporal autocovariance functions for two representative cases – fully coherent (Black phase screen) and nearly incoherent ($\gamma_\phi^2 = 16$ phase screen).

As can be seen in Figure 5, Figure 6, and from the data in Table 1, the PDFs are reasonably close with the left tail of the hot-air turbulence emulator cases being slightly lifted in comparison to the field test. Additionally, the correlation time, T_I , for the emulator is significantly reduced in comparison (2 ms vs. 6 ms, and 2.6 vs. 12.9 ms for the two represented cases, Black and 16 phase screens). This significant reduction in correlation time was also seen in [3] and could relate the fact that the hot-air turbulence emulator's C_n^2 is approximately 10,000 times stronger over 2 meters ($C_n^2 \sim 4 \cdot 10^{-11} \text{ m}^{-2/3}$) as compared to the C_n^2 from the two field tests ($C_n^2 \sim 1 \cdot 10^{-14} \text{ m}^{-2/3}$ and $C_n^2 \sim 10^{-15} \text{ m}^{-2/3}$ respectively for over the water and over the land).

From Table 1, comparing the number of fades of the two runs, 1622 and 1281 for the IR hot-air turbulence emulator run, and 294 and 416 for the over the water HeNe link it is notable that the stark

difference in number of fades may be linked to the correspondingly short correlation times. Specifically, 2 ms and 2.6 ms for the emulator, and 6 ms and 12.9 ms for the over the water field test. This relation was also seen in [3].

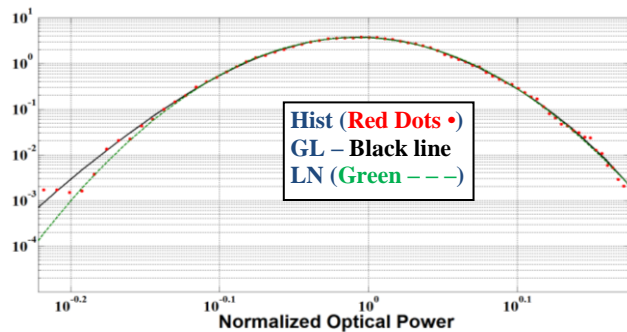
Also, from Table 1, the comparison of the 80% and 100% times for cumulative probability of channel fades is notable. The hot-air turbulence emulator had 80% of its fades occurring for about 2 ms or less with the longest fade occurring at 9 or 12 ms (Black and $\gamma_\phi^2 = 16$ phase screen cases respectively). This shortened correlation time in comparison with the over the water link which had an 80% point of 7 ms and 4 ms, and 100% point of 22 ms and 30 ms (Black and $\gamma_\phi^2 = 16$ phase screens respectively).

So, in summary of the results from Table 1, and Figures 5 and 6 – the PDF, scintillation index, and channel availability in the hot-air turbulence emulator are relatively comparable to the over the water field test but with a sizeable difference in number and duration of fades, as well as correlation times. These results lend additional support to the possible conclusion made in [3] that while 1st order statistics of intensity are vital, the 2nd order statistics of intensity could give valuable insight into the length and number of fades for the channel. Specifically, as discussed, the greatly reduced correlation time for the hot-air turbulence emulator appears to generally increase the overall number of fades but generally reduce the probability of a longer length fade.

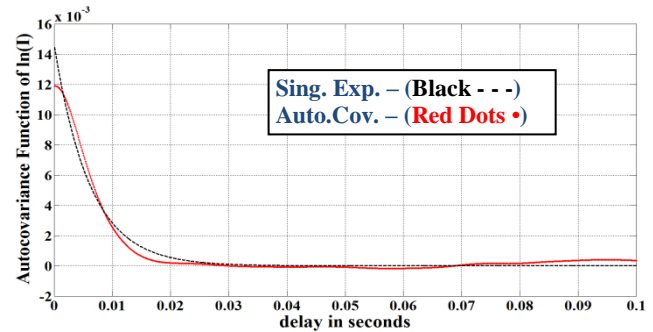
| Case | Approx. $\frac{D_s}{\rho_0}$ | σ_I^2 | N_f | Corr. time (ms) | No. of Fades | 80% and 100% cum. Prob. of fade times (ms) | Channel Avail. |
|--|------------------------------|--------------|-------|-----------------|--------------|--|----------------|
| Over creek, HeNe, 314 m (Fig. 2b), fully coherent (Black phase screen) | 0.2 | 0.012 | 0.1 | 6 | 294 | 7 to 22 | 98.1% |
| Turbulence emulator, IR, fully coherent (Black phase screen) | 0.3 | 0.014 | 1.0 | 2 | 1622 | 2 to 9 | 96.7% |
| Over creek, HeNe, 314 m, partially spatially coherent ($\gamma_\phi^2 = 16$) | 0.2 | 0.011 | 0.1 | 12.9 | 416 | 4 to 30 | 98.7% |
| Turbulence emulator, IR, partially spatially coherent ($\gamma_\phi^2 = 16$) | 0.3 | 0.010 | 1.0 | 2.6 | 1281 | 2 to 12 | 97.5% |

Table 1 – summary of USNA 314 m HeNe field test comparison with hot-air turbulence emulator

Note: Axis for the plots are the same in each figure for ease of comparison.

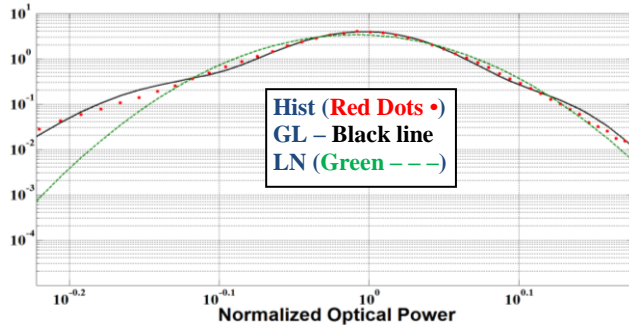


(a – 1)

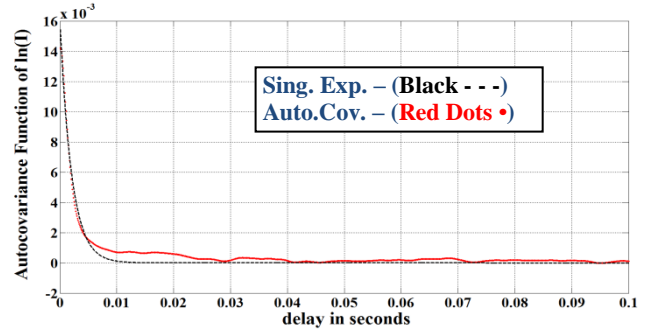


(a – 2)

(a) 314 m HeNe (632.8 nm) over creek link at USNA – (a-1) PDF, (a-2) Autocovariance

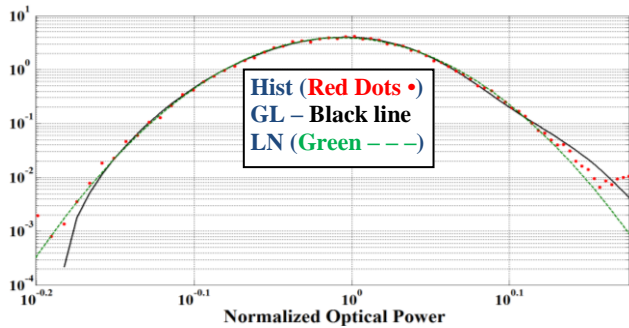


(b - 1)

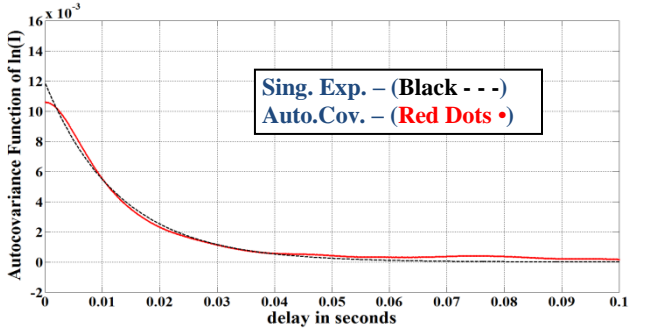


(b - 2)

(b) In laboratory hot-air turbulence emulator, IR (1550 nm) – (b-1) PDF, (b-2) Autocovariance
Figure 5 – Comparison of PDF, and temporal autocovariance 314 m HeNe laser beam propagation overwater and 2 m IR laser beam propagation through in-laboratory hot-air turbulence emulator for a fully coherent (Black phase screen) laser beam.

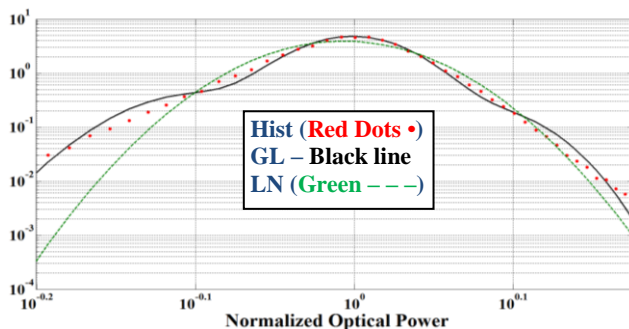


(a - 1)

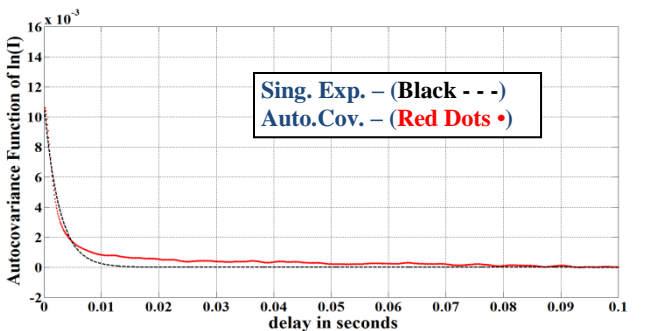


(a - 2)

(a) 314 m HeNe (632.8 nm) over creek link at USNA $\gamma_\phi^2 = 16$ phase screen – (a-1) PDF, (a-2) Autocovariance



(b - 1)



(b - 2)

(b) In laboratory hot-air turbulence emulator, IR (1550 nm) $\gamma_\phi^2 = 16$ phase screen – (b-1) PDF, (b-2) Autocovariance

Figure 6 – Comparison of PDF, and temporal autocovariance 314 m HeNe laser beam propagation overwater and 2 m IR laser beam propagation through in-laboratory hot-air turbulence emulator for a partially spatially coherent ($\gamma_\phi^2 = 16$ phase screen) laser beam.

Figure 7 shows a summary of results for the scintillation index, σ_I^2 , over varying degrees of spatial coherence using a HeNe laser and propagating over 314 m across the creek at the United States Naval Academy. The percent change between a given spatial coherence value and the fully spatially coherent (Black phase screen) propagation value is included (similarly for Figures 8 and 9). For example, there was 15.1% reduction in scintillation index when going from fully coherent HeNe propagation (Black phase screen) as compared with nearly incoherent propagation using a phase screen with a $\gamma_\phi^2 = 1$ (see Figure 1c for the phase screen used). Based on the 314 m propagation distance and atmospheric parameters, it appears that there could be a scintillation index ‘sweet’ spot around the partial spatial coherence associated with phase screen values of $\gamma_\phi^2 = 2$ and 64.

Figure 8 shows the same data comparison as in Figure 7 but for a field test with an IR (1550 nm) laser beam propagating 180 m over land. For this case, the strongest diffuser (most incoherent laser beam propagation) cases, $\gamma_\phi^2 = 1$ through 16, had higher scintillation indices than for the fully coherent (Black phase screen) propagation case. For these propagation parameters, there is a possible scintillation index ‘sweet’ spot around the partial spatial coherence associated with a phase screen value a γ_ϕ^2 of 32.

Figure 9 shows the same data comparison as Figures 7 and 8 but for an IR laser beam propagating 2 m through an in-laboratory hot-air turbulence emulator. For this data run, there was additional evidence of a potential scintillation index ‘sweet’ spot around the partial spatial coherence associated with phase screen values of $\gamma_\phi^2 = 4$ or 16. Based on these in-laboratory emulation results, seven additional experimental runs were performed for fully coherent propagation (Black phase screen), and six additional experimental runs at $\gamma_\phi^2 = 4$ and 16. The scintillation indices from the additional experimental runs were then compared using a two sample T-Test. Most introductory statistics books explain the use of the T-test to compare the statistical significance of the mean values between samples, see reference [17] for one text book. The p -values resulting from these computations were $p = 0.22$ for the phase screen value of $\gamma_\phi^2 = 4$ as compared with fully coherent propagation (Black phase screen) and $p = 0.02$ for the phase screen value of $\gamma_\phi^2 = 16$ as compared with fully coherent propagation (Black phase screen). These p -values shows no statistically significant difference (generally a p -value of 0.05 or less) for the $\gamma_\phi^2 = 4$ as compared with fully coherent propagation, but a strong statistically significant difference for the comparison of $\gamma_\phi^2 = 16$ with fully coherent propagation. The T-test results add additional strength to a potential scintillation index ‘sweet’ spot for partial spatial coherent laser beam propagation.

More testing and replication needs to done to validate these effects.

| γ_ϕ^2 (pixels ²) | σ_I^2 | % Diff. |
|---|--------------|------------|
| Black (Coherent, $\sim 512^2$) | 0.0119 | N/A |
| 1 (Strong diffuser) | 0.0101 | -15.1 |
| 2 | 0.0115 | -3.4 |
| 4 | 0.0107 | -10.1 |
| 8 | 0.0095 | -20.2 |
| 16 | 0.0107 | -10.1 |
| 32 | 0.0094 | -21.0 |
| 64 | 0.0095 | -20.2 |
| 128 (more weakly diffusing) | 0.0122 | 2.5 |

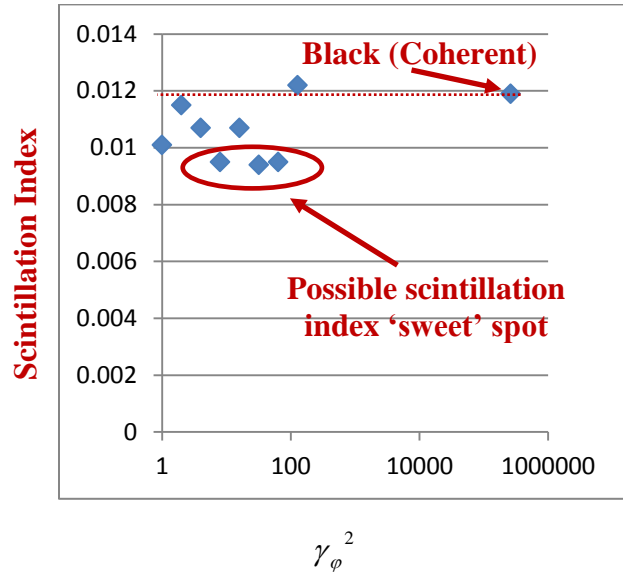


Figure 7 – Scintillation Index for HeNe laser beam propagation with a varying spatial coherence from fully coherent (Black phase screen) to nearly incoherent ($\gamma_\phi^2 = 1$) 314 m over water (Figure 2b) and with a $C_n^2 \sim 1 \cdot 10^{-14} \text{ m}^{-2/3}$.

| γ_ϕ^2 (pixels ²) | σ_I^2 | % Diff. |
|---|--------------|------------|
| Black (Coherent, $\sim 512^2$) | 0.0063 | N/A |
| 1 (Strong diffuser) | 0.0110 | 73.7 |
| 2 | 0.0121 | 91.1 |
| 4 | 0.0105 | 65.8 |
| 8 | 0.0102 | 61.1 |
| 16 | 0.0079 | 24.7 |
| 32 | 0.0057 | -10.0 |
| 64 | 0.0077 | 21.6 |
| 128 (more weakly diffusing) | 0.0074 | 16.8 |

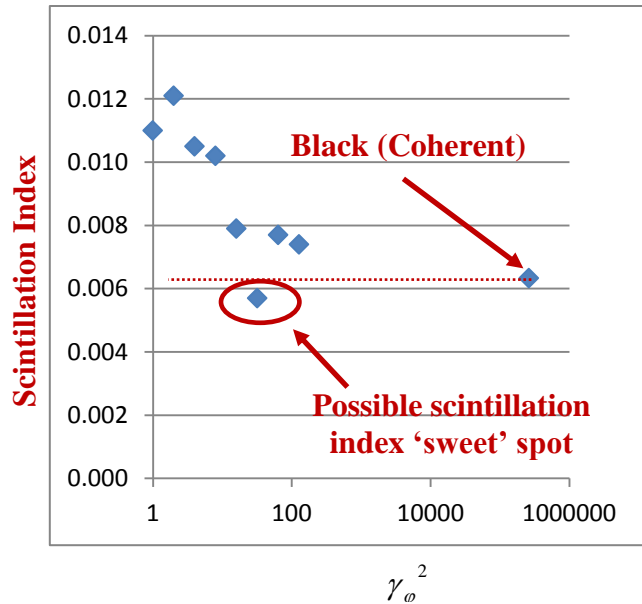


Figure 8 – Scintillation Index for IR laser beam propagation with a varying spatial coherence from fully coherent (Black phase screen) to nearly incoherent ($\gamma_\phi^2 = 1$) 180 m over land (Figure 2a) and with a $C_n^2 \sim 10^{-15} \text{ m}^{-2/3}$.

| γ_ϕ^2 (pixels ²) | σ_I^2 | % Diff. |
|---|--------------|------------|
| Black (Coherent, $\sim 512^2$) | 0.0111 | N/A |
| 1 (Strong diffuser) | 0.0134 | 20.4 |
| 2 | 0.0159 | 42.9 |
| 4 | 0.0096 | -13.7 |
| 8 | 0.0127 | 14.2 |
| 16 | 0.0099 | -11.0 |
| 32 | 0.0105 | -5.6 |
| 64 | 0.0190 | 70.8 |
| 128 (more weakly diffusing) | 0.0318 | 185.8 |

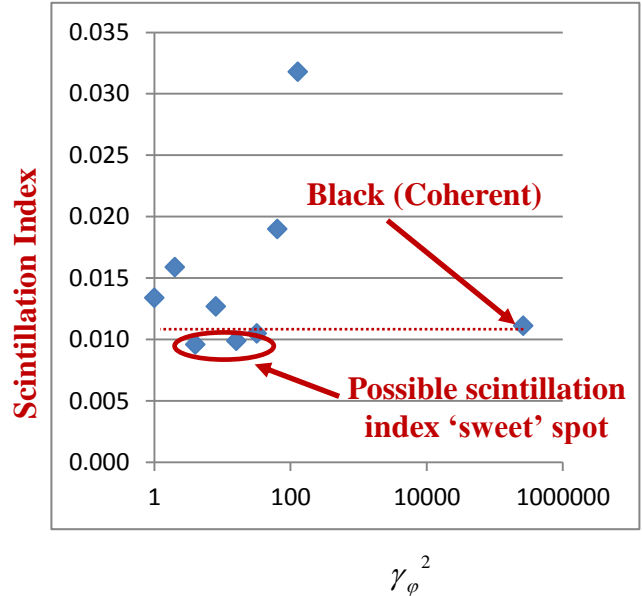


Figure 9 – Scintillation Index for IR laser beam propagation with a varying spatial coherence from fully coherent (Black phase screen) to nearly incoherent ($\gamma_\phi^2 = 1$) 2 m through an in-laboratory hot-air turbulence emulator with a $C_n^2 \sim 4 \cdot 10^{-11} \text{ m}^{-2/3}$. Note, the scintillation index values for Black and $\gamma_\phi^2 = 16$ were averaged over four and two runs respectively and all the others were single runs.

5. CONCLUSIONS

In summary, the 1st and 2nd order statistics through the single-point PDF, scintillation index, and temporal autocovariance function of the intensity of a HeNe laser beam propagating in the maritime environment over varying degrees of spatial coherence was compared with an IR laser beam propagated through an in-laboratory hot-air turbulence emulator. It was shown that while the PDFs were similar in comparison, but with a slightly lifted left tail for the turbulence emulation, the 2nd order temporal autocovariance correlation times differed quite markedly. From analysis of the fade statistics, a shorter correlation time appeared to correspond to a generally higher number of fades and a correspondingly shorter overall duration of fades. This finding is consistent with what was seen in [3]. Additionally, it was shown that there could be a potential scintillation index ‘sweet’ spot associated with a specific degree of partial spatial coherence of the laser beam and that it could be dependent on propagation distance, and atmospheric parameters.

6. REFERENCES

- [1] Mayer, K. J., Young, C. Y., "Effect of atmospheric spectrum models on scintillation in moderate turbulence," *J. Mod. Opt.* **55**, 1362-3044 (2008)
- [2] K. Drexler, M. Roggemann, D. Voelz, "Use of a partially coherent transmitter beam to improve the statistics of received power in a free-space optical communication system: theory and experimental results," *J. of Opt. Eng.*, 50(2), 025002, (2011).
- [3] C. Nelson, S. Avramov-Zamurovic, R. Malek-Madani, O. Korotkova, R. Sova, F. Davidson, "Measurements and comparison of the probability density and covariance functions of laser beam intensity fluctuations in a hot-air turbulence emulator with the maritime atmospheric environment," *Proc. SPIE* 8517, (2012)
- [4] O. Korotkova, S. Avramov-Zamurovic, R. Malek-Madani, and C. Nelson, "Probability density function of the intensity of a laser beam propagating in the maritime environment," *Optics Express*. Vol. 19, No. 21, (2011)
- [5] Barakat, R., "First-order intensity and log-intensity probability density functions of light scattered by the turbulent atmosphere in terms of lower-order moments," *J. Opt. Soc. Am.* **16**, 2269 (1999)
- [6] Aitchison, J. and Brown, J. A. C., [*The Lognormal Distribution*], Cambridge University Press, (1957)
- [7] Al-Habash, M. A., Andrews, L. C., and Phillips, R. L., "Mathematical model for the irradiance probability density function of a laser beam propagating through turbulent media," *Opt. Eng.* **40**, 1554-1562 (2001)
- [8] Andrews, L. C., and Phillips, R. L., [*Laser Beam Propagation through Random Media*, 2nd edition], SPIE Press, Bellingham, WA, (2005)
- [9] Pratap, R., [*Getting Started with MATLAB 7, a Quick Introduction for Scientists and Engineers*], Oxford University Press, (2006)
- [10] J. C. Ricklin, and F. M. Davidson, "Atmospheric optical communication with a Gaussian Schell beam," *J. Opt. Soc. Am. A*, Vol.20, No. 5 (2003)
- [11] J. C. Ricklin, and F. M. Davidson, "Atmospheric turbulence effects on a partially coherent Gaussian beam: implications for free-space laser communication," *J. Opt. Soc. Am. A*, Vol. 19, No. 9 (2002)
- [12] T. Shirai, O. Korotkova, and E. Wolf, "A method of generating electromagnetic Gaussian Schell-model beams," *J. Opt. A: Pure Appl. Opt.* **7**, 232-237 (2005)
- [13] Goodman, J. W., [*Introduction to Fourier Optics*, 2nd edition], McGraw-Hill Co. Inc., (1996)
- [14] Phillips, J. D., "Atmospheric Turbulence Simulation Using Liquid Crystal Spatial Light Modulators," Air Force Institute of Technology Masters Thesis, (2005)
- [15] Goodman, J. W., [*Introduction to Fourier Optics*, 2nd edition], McGraw-Hill Co. Inc., (1996)
- [16] Nelson, C., Avramov-Zamurovic, S., Korotkova, O., Malek-Madani, R., Sova, R., Davidson, F., "Probability density function computations for power-in-bucket and power-in-fiber measurements of an infrared laser beam propagating in the maritime environment," *Proc. SPIE* 8038, (2011)
- [17] Ross, S. M., [*Introductory Statistics*, 2nd Edition], Elsevier Inc., (2005)